Food Chemistry: X 25 (2025) 102084

Contents lists available at ScienceDirect

Food Chemistry: X

journal homepage: www.sciencedirect.com/journal/food-chemistry-x

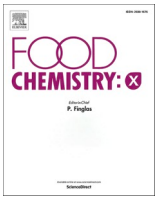

Quality, improvement of soluble dietary fiber from *Dictyophora indusiata* by-products by steam explosion and cellulase modification: Structural and functional analysis

Mengfan Lin [a,b], Changrong Wang [a,b], Wenfei Wu [a,b], Qingsong Miao [a,b], Zebin Guo [a,b,*]

[a] College of Food Science, Fujian Agriculture and Forestry University, Fuzhou, Fujian, PR China
[b] Integrated Scientific Research Base of Edible fungi Processing and Comprehensive Utilization Technology, Ministry of Agriculture and Rural Affairs, Fuzhou, Fujian, PR China

ARTICLE INFO

Keywords:
Steam explosion
Cellulase
Dictyophora indusiata
Soluble dietary fiber
Structural properties
Functional properties

ABSTRACT

Steam explosion (SE) and cellulase treatment are potentially effective processing methods for *Dictyophora indusiata* by-products, for use in high-value applications. The treatment conditions were optimized by response surface methodology, increasing the soluble dietary fiber (SDF) yield by 1.52 and 1.16 times after the SE and cellulase treatments, respectively. The both treatments did not affect the functional groups and crystal types of the polysachharides, but both reduced the crystallinity. The SDF had a porous microstructure, which would increase the specific surface area and facilitates the adsorption of water and glucose, thereby improving its functional properties. SE and cellulase treatment significantly improved the hydration capacity of SDF; the glucose adsorption capacity increased by 1.15 and 1.07 times, respectively. Overall, the modified SDF showed different degrees of advantages in terms of yield, physicochemical and functionality. This study demonstrated that SE and cellulase are effective modification methods for SDF made from *D. indusiata* by-products.

1. Introduction

Dictyophora indusiata (*D. indusiata*), also known as "bamboo fungus" and "bamboo ginseng", is an edible mushroom belonging to the genus Dictyophora (Wang et al., 2018), the subphylum Basidiomycotina, class Gasteromycetes, order Phallales, and family Phallaceae (Liao et al., 2015). It has a reputation as the "Queen of Mushrooms" (Hua et al., 2012); *D. indusiata* is rich in protein, minerals, vitamins, and various trace elements beneficial to human health, and it contains abundant biologically active components, such as polysaccharides, polyphenols, and flavonoids (Wu et al., 2022). *D. indusiata* by-products are mainly the discarded cap butt of *D. indusiata* from the actual production process. Therefore, efficient utilization of *D. indusiata* by-products is an important goal for the edible fungus industry, to reduce waste and generate new added-value products.

Dietary fiber (DF) is a carbohydrate polymer that is neither digested nor absorbed in the small intestine (Ma et al., 2022). The classification of SDF and IDF is based on the degree of solubility of the DF. Compared to IDF, SDF plays an important role in immunomodulatory activity and blood glucose regulation. SDF is a good raw material for producing gelling agents and emulsifiers, which are important functional ingredients of food products (Liu, Suo, et al., 2021; Liu, Zhang, et al., 2021). Although *D. indusiata*, is rich in DF, this primarily consists of IDF, which is less useful as a functional ingredient in processed food products (Chen et al., 2024). Therefore, industrially applicable methods to modify *D. indusiata* IDF into SDF would broaden its potential application in food processing.

The available modification methods for DF comprise physical, chemical and biological methods. The food-processing industry has made increasing use of steam explosion (SE), a physical modification method that is efficient, cost-effective and environmentally friendly. SE is economically viable, because of its high energy-conversion efficiency and relatively low energy consumption, compared with other physical methods (Wang et al., 2023). SE avoids the pollution issues associated with chemical treatment and addresses the inefficiency of extracting bioactive substances from raw materials. SE can also modify the physicochemical properties of SDF, making it a promising pretreatment method for extracting bioactive substances from plant-based raw materials. Both Shen et al. (2019) and Liu, Ao, et al. (2022) and Liu, Yu, et al. (2022) demonstrated that SE significantly increased the

* Corresponding author at: College of Food Science, Fujian Agriculture and Forestry University, Fuzhou, Fujian, PR China.
E-mail address: gzb8607@163.com (Z. Guo).

https://doi.org/10.1016/j.fochx.2024.102084
Received 10 September 2024; Received in revised form 28 November 2024; Accepted 8 December 2024
Available online 12 December 2024

physicochemical and functional properties of SDF. Furthermore, Yan et al. (2023) demonstrated that cellulase can improve the functional properties of DF with little change in the structure of the fiber. To our knowledge, there are previous reports on the extraction, structural characterization, and antioxidant capacity of *D. indusiata* polysaccharides, but fewer studies on modification of *D. indusiata* IDF. Therefore, SE and cellulase have considerable potential to modify DF extracted from *D. indusiata* by-products, thereby improving its quality and functional properties.

The objective of this study was to determine the optimal conditions for cellulase and SE modification of *D. indusiata* by-products IDF, as well as to assess the effect of these modifications on the structural and functional properties of the resulting SDF. This study provides a theoretical basis for expanding the application scope of SDF in the field of food processing, better meets the social demand for high-yield and high-quality SDF, and provides a theoretical basis for realizing the high-value utilization of *D. indusiata* by-products.

2. Materials and methods

2.1. Materials

D. indusiata by-products were provided by the Gutian Jianhong Agricultural Development Co.. Aladdin Biotechnology, located in Shanghai, China, provided heat-stable α-amylase (0.529 units/mg), protease (1.257 units/mg), and amyloglucosidase (266.8 units/mL). The *D. indusiata* by-products were modified using cellulase (Shanghai yuanye Bio-Technology Co., Ltd) and SE equipment (QB-200, Suzhou Qingzheng Ecological Technology Co., Ltd., Suzhou, China). All other chemicals used were of analytical grade.

2.2. Extraction of SDF from D. indusiata by-products

The SDF from *D. indusiata* by-products was extracted with some modifications from the previous method (Wang et al., 2024). Briefly, 1 g of 80-mesh dried *D. indusiata* by-products was mixed with 40 mL of 0.05 M MES-TRIS buffer and stirred until the powder was completely dispersed in the buffer. 790 uL of a-amylase was added and placed in a thermostatic shaking water bath (DF-101S, Henan Yuhua Instrument Co., Ltd.) at 95 °C for 35 min at 130 rpm. 100 uL of protease was added and the reaction was carried out in a thermostatic shaking water bath at 60 °C for 30 min at 130 rpm. A 3 mol/L acetic acid solution was added to decrease the pH to 4.5 ± 0.1, and the reaction was continued with the addition of 1000 uL of amyloglucosidase for 30 min. The enzyme suspension was centrifuged at 4000*g* for 15 min at room temperature using an L550 centrifuge (Hunan Xiangyi Experimental Instrument Development Co., Ltd.). Into the supernatant add four times the volume of warm 95 % ethanol (60 °C). After 24 h of standing at room temperature, the flocculent was obtained by rapid stirring and stored frozen at −80 °C. The precipitates were placed in a vacuum freeze dryer (FDU-1200, EYELA) and dried at a heating plate temperature of 60 °C, a cold trap temperature of −40 °C, and a vacuum of 80 Pa. The SDF was milled and stored at 4 °C.

2.3. Response surface methodology

2.3.1. Modification of D. indusiata by-products by steam explosion based response surface methodology

Modification of *D. indusiata* by-products using SE equipment. Response surface methodology (RSM) was used to assess the effects of SE pressure, residence time, and charge ratio on the SDF yield of *D. indusiata* by-products. Through single-factor experiments, RSM categorized SE pressures as high (+), medium (0), and low (−) levels at 0.75, 1.0, and 1.25 MPa; residence times at 10, 15, and 20 min; and charge ratios at 10 %, 30 %, and 50 %. Eq. (1) indicates that multiple regression analysis was performed on the BBD data using the second-order polynomial model. Table S1 displays the experimental values that were taken from the *D. indusiata* by-products SDF using the Box-Behnken design along with the matching projected values that came from using the second-order regression model.

$$Y = A_0 + \sum_{i=1}^{3} A_i X_i + \sum_{i=1}^{3} A_{ii} X_i^2 + \sum_{i=1}^{2} \sum_{j=i+1}^{3} A_{ij} X_i X_j \quad (1)$$

where Y is the dependent variable; A_0, A_i, A_{ii} and A_{ij} are model coefficients; and X_i and X_j are experimental variables at different levels.

2.3.2. Modification of D. indusiata by-products by cellulase based response surface methodology

Modification of *D. indusiata* by-products using cellulase. The effects of enzyme addition, enzyme treatment time and enzyme treatment pH on the SDF yield of *D. indusiata* by-products were evaluated using RSM. Based on single-factor experiments, RSM categorized enzyme additions as high (+), medium (0) and low (−) levels at 900, 1200 and 1500 U/g; enzyme treatment times at 4, 6 and 8 h; and enzyme treatment pH at 4.5, 5 and 5.5. The equations are the same as shown in 2.3.1 and the corresponding experimental values are shown in Table S2.

2.4. Structural properties analysis

2.4.1. Scanning electron microscopy

The surface microstructure of *D. indusiata* by-products SDF was observed using scanning electron microscopy (SEM, TESCAN MIRA4, Czech Republic). In brief, after being coated with gold powder, the dried SDF samples were placed to conductive adhesive and scanned under an objective aperture of 500 μm, a magnification of 1.00 kx, a working distance of 7.10 mm, and an accelerating voltage of 10 kV (Wang et al., 2024).

2.4.2. Fourier transform infrared spectroscopy (FT-IR)

The IR spectrograms of the three SDF samples were determined using a Nicolet iN 10 MX Fourier Transform Infrared Spectrometer (Thermo Scientific, USA). Briefly, samples weighing 150 mg of KBr and 1.5 mg of SDF were combined, pressed into a clear sheet, and scanned within the 4000–400 cm^{-1} wavelength region. The repetition period was adjusted at 32 scans per sample, with a 45 min background signal sampling interval and a 4 cm^{-1} resolution (Wei et al., 2022).

2.4.3. X-ray diffraction

The crystal structure of the samples was characterized using XRD (SmartLab, Japan). The device scans at 2°/min with 40 kV voltage and 40 mA current. XRD patterns were obtained by scanning and analyzing in the range of 10–35° (2θ) using a Cu-Kα radiation source (Ouyang et al., 2023).

2.4.4. Monosaccharide compositions

A Thermo ICS5000 ion chromatography system (ICS5000, Thermo Fisher Scientific, USA) was used to analyze and detect the monosaccharide fractions of SDF. Briefly, 1 mL of 2 M TFA solution was added to 5 mg of each SDF sample and heated at 121 °C for 2 h. Excess TFA was removed three times using nitrogen and methanol. In order to prepare the dried samples for injection into a high-performance anion-exchange chromatography system with pulsed amperometric detection, they were first dissolved in distilled water (HPAEC-PAD) (Zhu et al., 2021).

2.4.5. Thermogravimetric analysis

The thermal stability of SDF samples was measured using TGA (TGA 8000, China). 5 mg SDF samples were heated at a rate of 10 °C per minute to 700 °C while a nitrogen flow rate of 40 mL/min was maintained. The resulting weight loss was calculated. The differential thermogravimetric (DTG) curve was the thermogravimetric analysis (TGA) curve's first-order derivative (Huang et al., 2021).

2.4.6. Particle size analysis

A laser particle size analyzer (BT-9000ST) was used to measure the particle size distribution of SDF. An appropriate amount of SDF sample (refractive index 1.51) was taken and ethanol (refractive index 1.36) was used as a dispersant to achieve uniform dispersed with ultrasonic assistance. The particle size range was 10–1000 μm (Tang et al., 2023).

2.4.7. Specific surface area and pore diameter analysis

A fully automated specific surface area and pore analyzer (3Flex, Micromeritics, USA) was used to calculate the specific surface area (SSA), pore volume (PV), and pore size (PD) of SDF. Using N_2 as the adsorbed gas, gas molecules are adsorbed on the entire surface of the sample, and the specific surface area of the sample is determined by multiplying the number of adsorbed molecules by the molecular cross-sectional area (Wang et al., 2024).

2.4.8. Molecular weight analysis

The molecular weight of SDF was measured using gel permeation chromatography (GPC). Following accurately weighing 20 mg of SDF, 4 mL of mobile phase was added, and the mixture was allowed to dissolve for 10 min at room temperature before being filtered through a 0.45 μm microporous membrane for analysis. The chromatographic parameters were as follows: the mobile phase consisted of 0.1 M $NaNO_3$ aqueous solution, the column temperature was 40 °C, the injection volume was 50 μL, and the gel column was a Waters UltrahydrogelTM120 TM250 TM500 (7.8 × 300 mm). The detector was a G1362A contrast refractive detector (Zhang et al., 2024).

2.5. Functional properties analysis

2.5.1. Hydration properties

The hydration properties of *D. indusiata* by-products SDF were determined using the method of Xing et al. (2024) with slight modifications.

2.5.1.1. Determination of water holding capacity. Fill a centrifuge tube (W_1) with 0.5 g of the SDF sample (W). Stir in 10 mL of distilled water, then leave for 24 h at 25 °C. After centrifuging the sample for 10 min at 4000*g*, extract the supernatant and measure its mass (W_2). WHC was calculated as follows:

$$WHC(g/g) = \frac{W_2 - W_1}{W}$$

2.5.1.2. Determination of oil holding capacity. Fill a centrifuge tube (W_1) with 0.5 g of the SDF sample (W). After adding 10 mL of maize oil, stir for 24 h at 25 °C. After removing the top layer of oil and centrifuging for 15 min at 4000*g*, weigh the sample mass (W_2). OHC was calculated as follows:

$$OHC(g/g) = \frac{W_2 - W_1}{W}$$

2.5.1.3. Determination of swelling force. Weigh the SDF sample (W) to be 0.5 g, then combine it with 10 mL of distilled water. Note the mixture's initial volume (V_1). After 24 h of keeping the sample at 25 °C, note the mixture's ultimate volume (V_2). SC was calculated as follows:

$$SC(mL/g) = \frac{V_2 - V_1}{W}$$

2.5.2. Determination of cellulose, hemicellulose and lignin content

The neutral detergent fiber (NDF) and acid detergent fiber (ADF) were tested according to the method of Xing et al. (2024).

Using the following formulas, the contents of cellulose, hemicellulose, and lignin in SDF were determined:

Hemicellulose content : Hemicellulose (%) = NDF (%) − ADF (%)

Calculation of cellulose content : Cellulose = ADF (%)
− Residue after 72%sulfuric acid treatment (%)

Lignin content : Lignin (%)
= Residue after 72%sulfuric acid treatment (%)
− Ash after ashing (%)

2.5.3. Glucose adsorption capacity (GAC)

The GAC was determined using the method of Wang et al. (2024) with slight modification. After precisely weighing 0.2 g of the SDF sample, 20 mL of glucose solution containing varying concentrations (10, 50, 100, and 200 mmol/L) was added. The mixture was then kept in a water bath at 37 °C for six hours. After that, the supernatant was centrifuged for 15 min at 4000 r/min. The 3,5-dinitrosalicylic acid (DNS) technique was utilized to determine the concentration of glucose present in the supernatant. The GAC of SDF was calculated using the following formula:

$$GAC(mg/g) = \frac{C_1 - C_2}{M} \times V$$

where M is the mass of SDF (g), C_1 is the initial glucose concentration (mg/L), C_2 is the glucose concentration in the supernatant (mg/L), and V is the volume of glucose solution (L).

2.5.4. α-Amylase activity inhibitory ability (α-AAIR)

To determine the α-AAIR, the method of Tang et al. (2023) was used with slight modification. For one hour, 40 mL of 4 % potato starch solution were agitated at 37 °C with the addition of 4 mg of α-Amylase and 1 g of SDF. After centrifuging the mixture, the DNS method was used to determine the amount of glucose in the supernatant. The α-AAIR of SDF was calculated using the following formula:

$$\alpha - AAIR(\%) = \frac{C_C - C_S}{C_C} \times 100$$

where Cc and Cs are the glucose concentrations (mg/mL) in the supernatant with and without SDF, respectively.

2.5.5. Glucose dialysis retardation index (GDRI)

The GDRI was determined by reference to the method of Benitez et al. (2019) with minor modifications. 500 mg of SDF was put into a 15 cm dialysis bag (8000–14,000 Da) after being completely hydrated with 15 mL of glucose solution (100 mmol/L). The dialysis bag was incubated for two hours at 37 °C after being placed in a beaker with 200 mL of distilled water. Every 0.5 h, the dialysate's glucose concentration was determined using the DNS method. The GDRI of SDF was calculated using the following formula:

$$GDRI(\%) = \frac{C_C - C_S}{C_C} \times 100$$

where Cs is the glucose content (mmol/L) in dialysate with SDF; Cc is the glucose content (mmol/L) in dialysate without SDF.

2.6. Statistical analysis

All experiments were repeated three times, and the results were expressed as mean ± standard deviation. Data were analyzed for significance ($p < 0.05$) and response surface design using SPSS 27 and Design Expert 13 software, respectively. Graphing was performed using Orign 2024.

3. Results and discussion

3.1. Box-Behnken design

3.1.1. Regression fitting and analysis of variance (ANOVA)

Regression statistics of the parameter "SDF yield" from *D. indusiata* stalks were designed using Design Expert 13 software, (Tables S3, 4). Multiple regression was used to fit the data and obtain the quadratic polynomial regression eq. (2) for the response value, SDF yield (Y_1) against the factors SE pressure (A), residence time (B), and charge ratio (C), as well as the quadratic polynomial regression eq. (3) for the response value, SDF yield (Y_2) against the factors enzyme addition (D), enzyme treatment time (E), and enzyme treatment pH (F):

$$Y_1 = 0.3071 + 0.0079A + 0.0039B - 0.0029C - 0.0060AB + 0.0064AC + 0.0011BC - 0.0385A^2 - 0.0156B^2 - 0.0155C^2 \quad (2)$$

$$Y_2 = 0.2339 + 0.0040D + 0.0028E + 0.0028F - 0.0016DE - 0.0010DF - 0.0031EF - 0.0190D^2 - 0.0125E^2 - 0.0101F^2 \quad (3)$$

The regression model for The SE treatment has an F value of 51.01 ($p < 0.0001$), i.e., it is highly significant (Table S3). The model equation and the actual fitting error are minimal, and it can effectively show the relationship between the components and the response value, as indicated by the lack of fit term $P = 2.43$ (>0.05), which is not significant. The analysis shows that the effect of SE pressure on SDF yield is significant ($P < 0.05$), whereas the effects of SE residence time (A) and charge ratio (C) are not significant ($P > 0.05$). In addition, the quadratic terms of each factor are highly significant ($P < 0.01$) and the interaction terms AB and AC are significant ($P < 0.05$), whereas BC is not significant ($P > 0.05$). The extent of agreement between the regression model and the actual data is shown by the coefficient of determination (R^2). In this experiment, the values for R^2 (0.9850), R^2_{Adj} (0.9657), and R^2_{Pred} (0.8365) indicate that the model fit to the data is good, and the selected variables explained 96.57 % of the data. "Adequate precision" (Adeq prec) is a signal-to-noise ratio that compares the range of predicted values to the average prediction error; the Adeq prec of the model (20.08) denotes a sufficient signal (the ideal value is >4). With a cross-validation (CV) of 1.70 % (ideal value <5 %), the reproducibility of this experiment is good. The reliability of the second-order model is indicated by LoF = 0.2054.

This regression model for the enzyme treatment has an F value of 49.66 ($p < 0.0001$; Table S4), indicating that it is highly significant and robust. There is only a slight variation between the model equation and the fitted data, as indicated by the absence of fit term $p = 1.03$ (>0.05), which is not statistically significant. The analysis showed that the effect of enzyme addition on SDF yield was highly significant ($P < 0.01$), and that the effects of enzyme treatment time and enzyme treatment pH on the SDF yield was significant ($P < 0.05$). In addition, the quadratic terms of all factors were highly significant ($P < 0.01$), while the interaction terms were non-significant ($P > 0.05$). $R^2 = 0.9846$, $R^2_{\text{Adj}} = 0.9648$, and $R^2_{\text{Pred}} = 0.8791$, indicating that the model is well-fitted to the data. The chosen criteria influenced 96.48 % of the trial results. Adeq prec = 19.4676 indicates an adequate signal. The C.V.% is 1.25 % (<5 %), signifying good repeatability of the experiment. The reliability of the second-order model is indicated by LoF = 0.4701.

3.1.2. Response surface analysis

The relationship between the variable factors and response values, and the interactions between pairs of factors, are intuitively represented by response surfaces and contour plots. The greater the effect of the factor on the response value, the steeper the surface of the response surface plot. The closer the shape of the contour line is to a circle, the weaker the interaction between the two factors.

The SDF yield obtained from extraction of *D. indusiata* by-products increased, then decreased with increases in SE pressure, residence time, and charge ratio (Figs. S1a–c). Lower pressures apparently have little effect on the structure of DF, but too high a pressure appears to degrade cellulose and lignin into small molecules, which are very soluble and not recovered by alcohol precipitation. Extending the SE residence time allows the raw material in the IDF to be maximally hydrolyzed to SDF, but excessive residence time appears to degrade cellulose and lignin into small molecules. A low charge ratio lowers the SDF yield, because there is little DF to modify, but a high charge ratio results in tight packing of the raw material, inhibiting the steam from penetrating into the cellular structure and causing incomplete tissue disruption. The contour plots of residence time with charge ratio and the interaction of SE pressure with residence time are elliptical (Figs. S1d–f), suggesting that there is a strong interaction between these parameters. The SE pressure and charge ratio contour plots, however, are close to circular, indicating a weak interaction between them, in agreement with the ANOVA results.

The SDF yield from *D. indusiata* by-products increased then decreased with increased enzyme addition, enzyme treatment time, and treatment pH (Figs. S1g–i). Cellulase can degrade IDF in the by-products of *D. indusiata*, acting on the β-1,4 glycosidic bond of cellulose, cutting off the molecular chain, degrading crystalline cellulose into amorphous cellulose, decreasing the molecular weight, increasing the solubility, and prompting its transformation into SDF. When the amount of cellulase added exceeds a certain level, it will lead to the continued degradation of SDF into smaller-molecular-weight sugars, such as oligosaccharides and monosaccharides, which cannot be precipitated by alcohol because of their small size. With the prolongation of enzymatic time, the interaction between cellulase and the *D. indusiata* by-products IDF became more adequate, and the SDF obtained from degradation increased. However, as the duration of the reaction increased, the enzyme-substrate interaction grew closer to saturation, resulting in a drop in IDF concentration and an increase in SDF content.

The effect of the feedback inhibitory mechanism on the cellulase increased, resulting in reduced enzyme efficiency, a decrease in reaction rate, and further degradation of SDF by cellulase. Enzyme activity and stability were significantly affected by pH. A reaction system that is too acidic or too alkaline changes the enzyme protein conformation, resulting in reduced enzyme activity, or even denaturation and inactivation. In addition, at low pH, the glycosidic bond of SDF is easily cleaved by a non-enzymic, acid-catalyzed reaction, resulting in a low yield of SDF. The SDF yield was highest at pH 5.0, indicating that this pH is the optimum value for enzyme activity. The contour plots between pH and SDF yield are nearly elliptical (Figs. S1j–l), indicating that the interaction between them is strong, which is also consistent with the ANOVA results.

3.1.3. Optimization of SE and cellulase modification process and validation

According to Design Expert 13 analysis, the optimal SE conditions were an SE pressure of 1.0 MPa, residence time of 15.5 min, and charge ratio of 28.6 %; the predicted SDF yield under these conditions was 0.308 g. The actual experimental yield of SDF under the optimum conditions was 0.311 ± 0.02 g, very close to the predicted yield and 1.52 times that from non-SE treated raw material.

The predicted optimal cellulase modification conditions were an enzyme addition of 1230 U/g, a treatment time of 6.2 h and a treatment pH of 5.0; the predicted SDF yield under these conditions was 0.234 g. The actual yield of SDF under the optimal conditions was 0.236 ± 0.03 g, very close to the predicted yield and 1.16 times that from non-cellulase treated material. The relative standard errors between the actual and predicted values, were 0.85 % (<10 %) and 0.96 %, respectively, demonstrating the precision and accuracy of the regression model.

3.2. Structural properties

3.2.1. SEM

The microstructures of the *D. indusiata* DF, both before and after treatment, were observed by SEM (Fig. 1). Unmodified SDF (O-SDF) had a dense structure and a smooth surface. Small amounts of protein and starch particles adhering to the surface appear to form lumps and globules (Wen et al., 2017). The resulting SDF (S-SDF), a *D. indusiata* by-products modified by SE, was structurally disrupted. During the final depressurization stage of the SE process, the steam/water absorbed by the *D. indusiata* by-products tissue undergoes a very rapid expansion, which disrupts the tissue and ruptures the cellular structure, resulting in roughness of the SDF particle surface and the appearance of honeycomb-like pores. Cellulase treatment promoted the rupture and segregation of the SDF surface, so that the cellulase-treated *D. indusiata* by-products SDF (*E*-SDF) surface also appeared to have a distinct pore-like structure, as seen in Fig. 1e and f as well. The structural changes induced by SE and cellulase expose more groups to SDF, thus providing more sites for other solvents to interact with it (Yang et al., 2022).

3.2.2. FT-IR

The FT-IR spectra of *D. indusiata* by-products SDF, both before and after treatment were recorded (Fig. 2). SDF before and after modification had similar spectral indicating that they contained essentially the same functional groups, albeit in different amounts, and all of them exhibited the characteristic peaks of polysaccharides. The hydroxyl group in the crystalline region of cellulose accounts for the O—H stretching vibration, at 3300 cm^{-1} (between 3200 and 3650 cm^{-1}) (Wen et al., 2017). After SE and cellulase treatment, the absorption intensity near 3300 cm^{-1} was slightly reduced, indicating that the intermolecular hydrogen bonding in the cellulose crystalline region was disrupted, and soluble sugars and amorphous cellulose were produced (Liu, Suo, et al., 2021; Liu, Zhang, et al., 2021). The appearance of absorption peaks at 1656 cm^{-1} is attributed to the stretching vibration of C═O (Xu et al., 2019). The SE and cellulase treatments, degraded hemicellulose and lignin, weakening the intensity of the S-SDF and *E*-SDF peaks. Notably, the primary component of IDF is lignin, indicating that the degradation of IDF is responsible for the rise in SDF content of *D. indusiata* by-products during the SE and cellulase treatments (Wang et al., 2024).

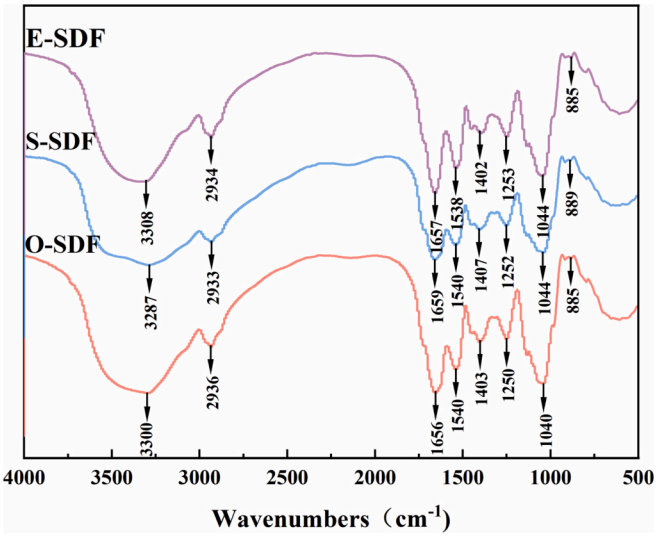

Fig. 2. FT-IR spectra of O-SDF, S-SDF and E-SDF.

The peak at 885 cm^{-1} (near 890 cm^{-1}) indicating β-glycosidic bond stretching vibration was visible in the spectra of all three SDF fractions. The intensity of the 885 cm^{-1} peak was lower in the S-SDF and E-SDF spectra than that of O-SDF, indicating that the DF polymer chains were degraded by SE and enzymic hydrolysis (Gu et al., 2020). In summary, compared to O-SDF, the intensity of the absorption peaks of S-SDF and E-SDF decreased to different degrees. This indicates that the modification led to the destruction of the chemical groups in SDF, a reduction in the intermolecular hydrogen bonding force of SDF, and the degradation of some macromolecular substances.

3.2.3. XRD

The XRD patterns of *D. indusiata* by-products SDF before and after the treatments were recorded (Fig. 3). There was no significant difference in the positions of the diffraction peaks of O-, S- and *E*-SDF before and after the treatments, indicating that there was no change in the crystalline form induced by the treatments. There were intense diffraction peaks at

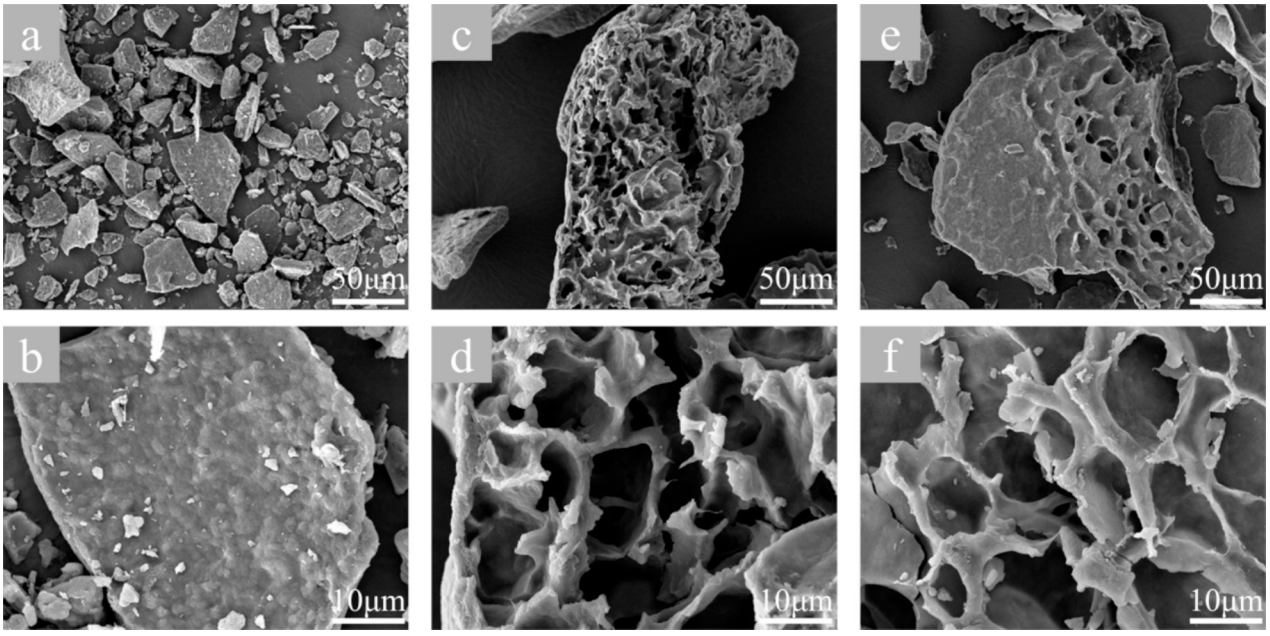

Fig. 1. Scanning electron microscopy (SEM) images (magnification 1.00 k and 5.00 k, scale bar 50 and 10 μm, respectively) of three SDFs from *D. indusiata* by-products. (a–b) O-SDF, (c–d) S-SDF and (e–f) E-SDF.

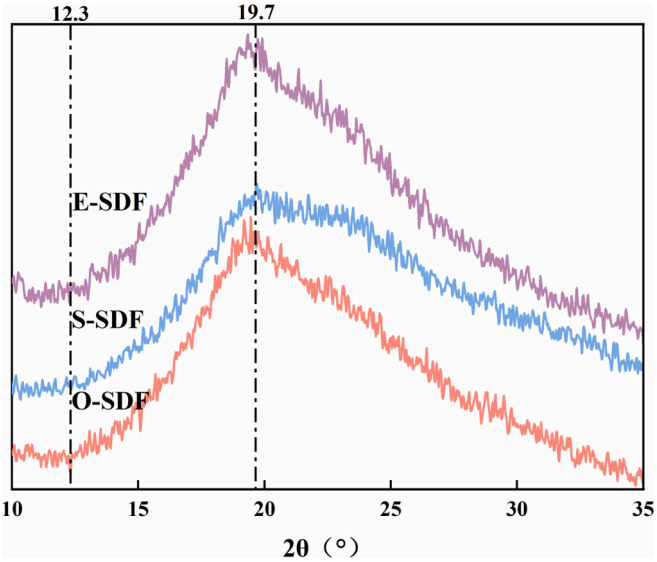

Fig. 3. XRD of O-SDF, S-SDF and E-SDF.

12.3° and 19.7° (2θ), indicating that the crystal structure of the SDFs was of cellulose type I (Khawas & Deka, 2016), with the coexistence of crystalline and amorphous regions. Compared with O-SDF, the crystallinity of S-SDF and E-SDF decreased from 17.0 % to 7.1 % and 5.7 %, respectively, indicating that the crystalline regions of the cellulose structure were disrupted. Combined with the FT-IR analysis, the intensity of the absorption peaks was slightly reduced, and the intermolecular hydrogen bonding in the crystalline regions was disrupted, enhancing the disordered regions. Xi et al. (2023) investigated the effect of *SE*-assisted extraction on the structure of DFs in highland barley bran, and they found that SE reduced the degree of crystallinity, which is due to the fact that the mechanical factors reduce the degree of polymerization, which is consistent with this study. Cellulase can act on the β-1-4 glycosidic bond of cellulose to degrade crystalline cellulose into amorphous cellulose and produce soluble cellulose degradation products (Cao & Tan, 2005), which changes the crystalline regions of SDF from an ordered state to a disordered, amorphous state.

3.2.4. Monosaccharide compositions

The monosaccharide compositions of *D. indusiata* by-products O-, S- and *E*-SDF were determined (Fig. 4); they were mainly composed of fucose, galactose, glucose, and mannose, with glucose and mannose being the predominant monosaccharides. The relative contents of the monosaccharides changed after SE and cellulase treatment, in

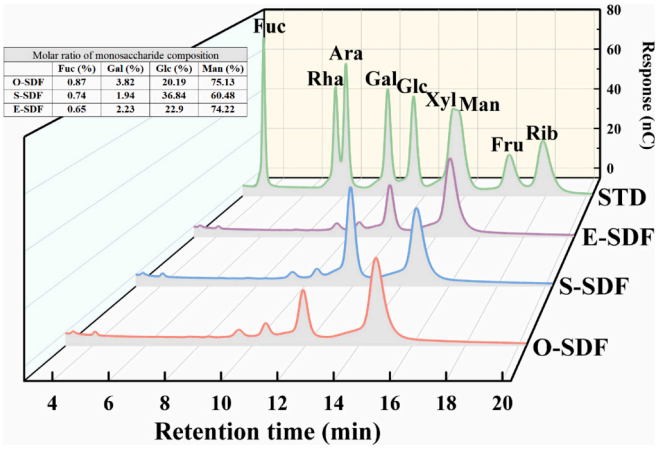

Fig. 4. Monosaccharide compositions of O-SDF, S-SDF and E-SDF.

agreement with a previous report (Pan et al., 2023). The degradation of cellulose, hemicellulose, and lignin to low MW monosaccharides and oligosaccharides increases the proportion of glucose residues in the modified SDF (Shen et al., 2020). Nevertheless, the monosaccharide content of some low-molecular-weight sugars may decrease because of further degradation to smaller molecular products that are not precipitable by alcohol. Since glucose is the dominant component of cellulose (Ouyang et al., 2023), the higher glucose content in S-SDF and *E*-SDF than in O-SDF suggests that cellulose hydrolysis transformed part of the IDF in the cell wall into soluble fiber rich in β-glucose (Yang et al., 2022).

3.2.5. TGA

The TGA and DTG curves of O-, S-, and E-SDF before and after modification were determined (Fig. 5a–c). The three TGA curves showed a three-stage weight loss between 30 and 700 °C. In the first stage, the weight losses of O-SDF, S-SDF, and E-SDF were 8.08 %, 6.75 %, and 6.60 %, respectively, and the corresponding temperatures were 156, 151 and 146 °C, respectively. At this stage the weight losses result from the loss of free or bound water from the DF. The second weight loss stage was between 200 and 500 °C, resulting from the decomposition of thermally unstable functional groups (Liu, Ao, et al., 2022; Liu, Yu, et al., 2022). At this stage, cellulose and hemicellulose combustion cleavage and breakage of polysaccharide chains and hydrogen bonds lead to rapid loss of mass, as reported by Johar et al. (2012). Finally, the process of thermal decomposition of carbon dominates when the temperature exceeds 500 °C until the end of combustion (Huang et al., 2021). Lignin exhibits slow but continuous pyrolysis between 200 and 700 °C (Liu, Suo, et al., 2021; Liu, Zhang, et al., 2021). At the completion of the heating cycle, the final weight losses of O-SDF, S-SDF, and *E*-SDF were 15.72, 24.91, and 21.26 %, respectively. These results suggest that the SE and enzyme treatments increased the thermal stability of the DF, consistent with a previous report (Wang et al., 2024) on SE improvement in *Tremella fuciformis* stem DF. The DTG curves show that the peak temperature has increased. There are more short-chain polysaccharide chains in the treated DF than in the untreated DF; the strong intramolecular hydrogen bonds in the short-chain species increase their stability (Chen et al., 2014). Increased thermal stability would widen the applicability of *D. indusiata* by-products SDF in cooked food products, such as baked products.

3.2.6. Particle size and SSA

The particle size and SSA of *D. indusiata* by-products SDF before and after modification were determined (Table 1 and Fig. 6a). Smaller particle sizes correlate with increased solubility in the food matrix, higher dispersibility of the material, and more particles per unit weight (Ren et al., 2021). The median particle size (D_{50}) of O- SDF was 27.6 μm, and S- and E-SDF had smaller D_{50} values. The difference between D[3,2] and D[4,3] became smaller, indicating a more regular and concentrated particle shape distribution. The uniformity of the DF particle size distribution can be reflected by the span. As the span value decreases, it becomes apparent that the cellulase treatment and SE have improved the detail and uniformity of the SDF powder.

N_2 adsorption was used to measure the surface area and pore size of the DF particles. After treatment, the *D. indusiata* by-products SDF had a larger PD and PV, and the SSA increased, consistent with the SEM observations. During the pressure release stage of SE treatment, the water inside the tissues flashes into steam, causing the internal structure to become loose and porous, facilitating access for the cellulase enzyme, which further degrades the structure of the DF, resulting in a wrinkled and porous surface and a higher SSA. The reduction in particle size also exposes more hydroxyl, carbonyl, and other functional groups (Jiang et al., 2022), which increases the contact between the enzyme and its sites of action and thus promotes the enzymatic degradation of DF (Wen et al., 2017). Enzymic and physical treatments reduce the particle size of SDF, suggesting that these changes would affect its adsorption capacity. Luo et al. (2018) reported that enzymatic and physical treatments

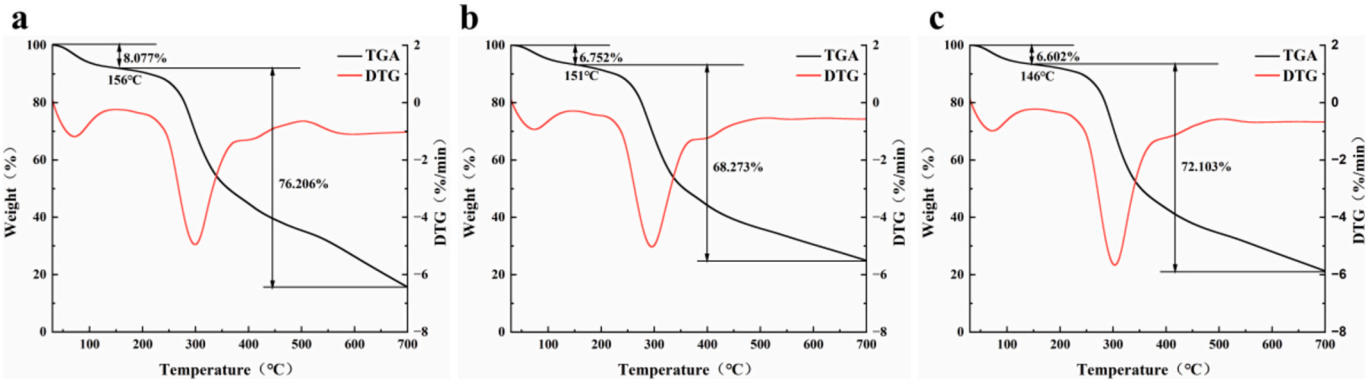

Fig. 5. (a–c) Thermogravimetric analysis curves of O-SDF, S-SDF and E-SDF.

Table 1
The particle size of the SDF of *D. indusiata* by-products.

	D[3,2]/μm	D[4,3]/μm	D10/μm	D50/μm	D90/μm	Span
O-SDF	15.91 ± 0.11^{a}	33.30 ± 0.10^{a}	6.81 ± 0.08^{a}	27.60 ± 0.08^{a}	69.80 ± 0.11^{a}	2.28 ± 0.00^{a}
S-SDF	6.20 ± 0.23^{b}	7.27 ± 0.07^{b}	3.83 ± 0.14^{c}	6.93 ± 0.10^{b}	11.20 ± 0.14^{b}	1.06 ± 0.06^{b}
E-SDF	6.53 ± 0.07^{b}	7.25 ± 0.10^{b}	4.43 ± 0.14^{b}	6.98 ± 0.10^{b}	10.60 ± 0.13^{c}	0.88 ± 0.03^{c}

Values in the same column with different letters are significantly ($p < 0.05$) different.

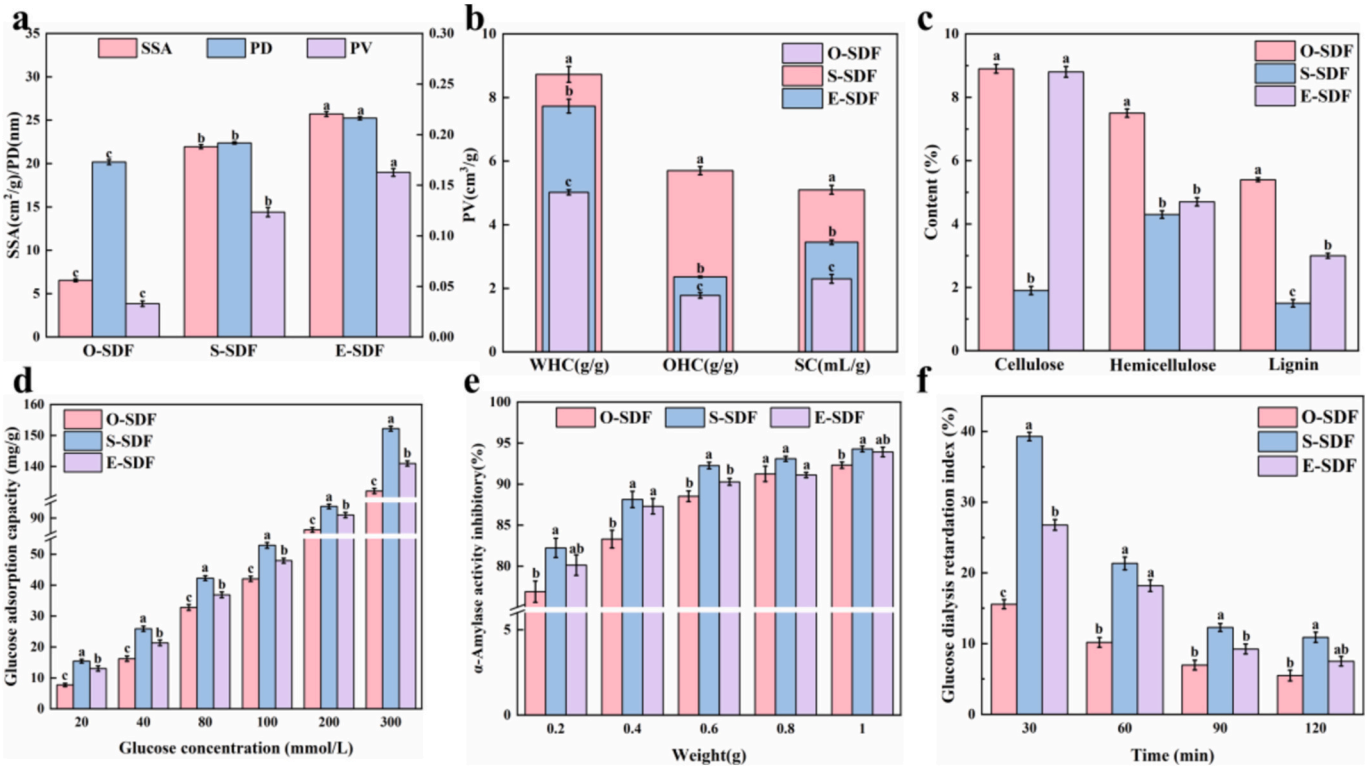

Fig. 6. (a–f): (a) Pore diameter (PD), pore volume (PV) and specific surface area (SSA) of O-SDF, S-SDF and E-SDF, (b) The water holding capacity (WHC), oil holding capacity (OHC), and swelling capacity (SC) of O-SDF, S-SDF and E-SDF, (c) the cellulose, hemicellulose and lignin content of O-SDF, S-SDF and E-SDF, (d) Glucose adsorption capacity of O-SDF S-SDF and E-SDF, (e) α-Amylase inhibitory ability of O-SDF S-SDF and E-SDF, (f) Glucose dialysis retardation index of O-SDF S-SDF and E-SDF.

significantly reduced the particle size and formed a larger specific surface area of BIDF, and that these structural changes improved the functional properties of BIDF such as WHC and GAC.

3.2.7. *Molecular weight*

The average MWs of *D. indusiata* by-products SDF before and after treatment were determined (Table 2). According to studies, the degree of polymerization is lower, the solubility is better, and the viscosity is lower when the Mw is smaller. The MW dispersion coefficient indicates the range of the MW distribution (Shen et al., 2020). The weight-average Mw and dispersion coefficient of SDF treated with SE and cellulase are significantly lower than those of O-SDF. This indicates that the Mw of

Table 2
Molecular weight of of O-SDF, S-SDF and E-SDF.

	Mw (g/mol)	Mn (g/mol)	Mw/Mn
O-SDF	6.03×10^5	1.61×10^5	3.74
S-SDF	4.26×10^5	1.24×10^5	3.45
E-SDF	5.91×10^5	1.71×10^5	3.46

SDF is reduced and the Mw distribution is relatively concentrated and uniform. This is consistent with the action of SE and cellulase disrupting intermolecular interactions and separating bound macromolecules and degrading longer polysaccharide chains into shorter ones (Tang et al., 2023). Shen et al. (2020) found that lower Mw SDFs typically have better functional activity, better solubility, and lower viscosity.

3.3. Functional properties

3.3.1. Hydration properties

The WHC, OHC, and SC results of *D. indusiata* by-products SDF before and after modification were determined (Fig. 6b). WHC depends on the structure of SDF and the amount of hydrophilic components such as cellulose and hemicellulose (Xi et al., 2023), which can change the viscosity of food products and prevent them from shrinking. Both treatments enhanced the hydration properties of SDF; SE increased the WHC, OHC and SC by 1.73-, 3.2- and 2.2-fold, respectively, and cellulase increased the WHC, OHC and SC by 1.5-, 1.3- and 1.5-fold, respectively. The porous surface structure resulting from the treatments would be expected to increase the exposure of free hydroxyl groups, generating more water-binding sites and increasing the WHC and SC (Kong et al., 2020). The β-glycosidic linkages between cellulose and hemicellulose are cleaved by cellulase hydrolysis of DF, causing additional hydrogen-bonded and dipolar forms to emerge (Gu et al., 2020). Disruption of the crystalline regions of the cellulase-modified DF and the generation of new amorphous regions facilitate permeation of water into the fiber structure, increasing its WHC and SC. The assessment of DF's ability to absorb lipophilic components often considers its ability to bind to lipids, specifically cholesterol. A high OHC retains oil more effectively during food processing and absorbs cholesterol in the intestinal lumen, which reduces intestinal absorption of cholesterol and lowers blood cholesterol levels ((Liu, Suo, et al., 2021; Liu, Zhang, et al., 2021). The high SSA and porosity of the S-SDF surface structure promote the adhesion of oil and help increase the OHC and SC, whereas the dense multilayered structure of the O-SDF reduces them.

3.3.2. Cellulose, hemicellulose, and lignin content

The cellulose, hemicellulose, and lignin contents of *D. indusiata* by-products SDF before and after were compared (Fig. 6c). Cellulose, hemicellulose, and lignin in DF are cross-linked by hydrogen bonds and chemicals (Jiang et al., 2017); the mechanical degradation applied by SE disrupts the cross-links between the three components (Tanpichai et al., 2019), thereby increasing the SDF yield. Cellulase hydrolysis cleaves glycosidic bonds in DF polysaccharides and degrades lignin, by cleaving the β-O-4′ bonds in the lignin structure (Li et al., 2007). It can be seen from the figure that both modification methods significantly reduced the cellulose, hemicellulose, and lignin content of SDF. This agrees with the findings of others. Tang et al. (2023) found that the contents of all three substances in adlay bran SDF were significantly reduced after SE treatment. Xing et al. (2024) reported that because of differences in the chemical stability of cellulose, hemicellulose, and lignin, the contents of the three substances were significantly reduced under SE conditions of 1.0 MPa in 90 s, and that the contents of the three substances appeared to be reduced to different degrees.

3.3.3. GAC

GAC is a vital property, which indicates the capacity of DF to bind glucose in the gastrointestinal tract and slow its absorption into the bloodstream (Xing et al., 2024). The GACs of *D. indusiata* by-pridects SDF before and after treatment were compared (Fig. 6d). The GAC of all three SDFs was high and *E*-SDF had the highest GAC, which would confer the highest capacity to lower postprandial hyperglycemia. The treatments, as shown by the SEM and particle size analyses above, increase the surface area and porosity, thereby increasing the abundance of glucose binding sites and the GAC. Treatment of DF by SE and cellulase exposes more functional groups on the fiber surface that can interact with glucose (Yu et al., 2018), such as phenolic groups with stronger binding affinity to glucose. Zheng et al. (2021) showed that DF containing higher polyphenol content has higher glucose-binding capacity. Therefore, the high GAC values of S-SDF and *E*-SDF may also be due to SE and cellulase treatments exposing more phenolic groups on the fiber surface.

3.3.4. α-AAIR

The α-AAIR of DF is an important indicator of its capacity to inhibit the digestion of starch into glucose. The α-AAIR values of *D. indusiata* by-products SDF before and after treatment were determined (Fig. 6e). The two modified SDFs showed higher α-amylase inhibition than O-SDF. The physical barrier established by SDF molecules decreases the accessibility of α-amylase to starch molecules adsorbed into the fiber lattice, which is the primary cause for the inhibitory effect of SDF on α-amylase (Zheng et al., 2021). Because of its poor crystallinity and porous honeycomb shape, α-amylase is less able to operate since more active chemicals and functional groups can bind to it more easily.

The GAC of SDF also affects α-amylase inhibitory activity, since SDFs with a high GAC can inhibit contact between starch and α-amylase by binding to starch molecules (Ma & Mu, 2016). Yang et al. (2022) investigated three modification methods and found that the SDFs obtained from all three modification methods showed better inhibitory activity against α-amylase. Therefore, the *D. indusiata* by-products SDF has great potential for glycemic control after modification.

3.3.5. GDRI

The GDRI is an indicator of the capacity of DF to inhibit and delay absorption of glucose from the gastrointestinal tract, thereby reducing the glycemic index of the food. The GDRI values of *D. indusiata* by-products SDF before and after treatment were determined (Fig. 6f). The GDRI values of the S-SDF and E-SDF fractions were markedly higher than those of the O-SDF, but these values gradually declined with time. This is in agreement with the results of Huang et al. (2019) in their study on the effect of extrusion treatment on the hypoglycemic capacity of fiber-rich orange pomace. GDRI is related to the functional groups, molecular structure and GAC of the SDF (Zheng et al., 2021). Some functional groups, such as aldehydes, have a strong binding affinity for glucose, thereby inhibiting glucose absorption (Yan et al., 2023). The increased GDRI values of S-SDF and E-SDF appear to result from their porous surface structures, as shown by SEM, and their high GAC. The porous structure makes it easier for glucose molecules to enter the interior of the fibers and increases the abundance of glucose binding sites, which increases the adsorption capacity of SDF for glucose (Ren et al., 2021). These results suggest that the modified SDF has a higher capacity to delay the absorption of glucose from the gastrointestinal tract.

4. Conclusion

This study investigated the effects of SE and cellulase treatments on the extraction yield, and structural and functional properties of DF obtained from *D. indusiata* by-products. Both treatments significantly increased the yield of DF. It was shown that the increase in SDF yield by SE and cellulase was mainly through the destruction of glycosidic bonds in fiber macromolecules, which promoted the degradation of cellulose, hemicellulose, and lignin. The SE treatment reduced the cellulose, hemicellulose, and lignin contents of the DF by 78.7, 42.7 and 72.2 %,

respectively. SE and cellulase treatment also disrupted the hydrogen bonding within the crystalline regions of the SDF structure, weakening the intermolecular forces, forming a loose and porous SDF surface, which increased its specific surface area, and its glucose adsorption capacity. SE and cellulase increased the water holding capacity of DF from 5.02 ± 0.08 g/g to 8.73 ± 0.25 g/g and 7.73 ± 0.22 g/g, respectively. The lower MWs of the SDF molecules increased their glucose adsorption capacity, which would increase their capacity to delay glucose absorption from the gastrointestinal tract, thereby decreasing the glycemic index of the food. The treatments increased the thermal stability of *D. indusiata* by-products SDF, which increases its potential for application in thermal food processing, such as baking. In summary, the SE and cellulase treatments are effective tools for expanding the range of applications of *D. indusiata* by-products and achieving high-value utilization. This study provides a theoretical basis for exploring the modification of SE and cellulase as by-products of edible-mushroom processing.

Further studies are necessary to explore the effects of SE and cellulase-modified SDF on the intestinal flora by simulated in vitro fermentation, to elucidate the mechanism of the DF influence on the composition and function of the intestinal microflora and to develop functional products.

CRediT authorship contribution statement

Mengfan Lin: Writing – original draft, Investigation, Formal analysis, Data curation, Conceptualization. **Changrong Wang:** Software, Methodology, Investigation. **Wenfei Wu:** Writing – review & editing, Supervision. **Qingsong Miao:** Writing – review & editing, Supervision. **Zebin Guo:** Writing – review & editing, Writing – original draft, Validation, Supervision, Resources, Project administration, Investigation, Funding acquisition, Conceptualization.

Declaration of competing interest

The authors declare that they have no known competing financial interests or personal relationships that could have appeared to influence the work reported in this paper.

Data availability

Data will be made available on request.

Acknowledgments

This study was supported by the Special Fund for Young Top-Notch Talents of “Young Eagle Program” in Fujian Province (Minwei Talent [2021] No. 5). The authors acknowledge the assistance of Instrumental Analysis Center of Fujian Agriculture and Forestry University.

Appendix A. Supplementary data

Supplementary data to this article can be found online at https://doi.org/10.1016/j.fochx.2024.102084.

References

Benitez, V., Rebollo-Hernanz, M., Hernanz, S., Chantres, S., Aguilera, Y., & Martin-Cabrejas, M. A. (2019). Coffee parchment as a new dietary fiber ingredient: Functional and physiological characterization. *Food Research International, 122*, 105–113. https://doi.org/10.1016/j.foodres.2019.04.002

Cao, Y., & Tan, H. (2005). Study on crystal structures of enzyme-hydrolyzed cellulosic materials by X-ray diffraction. *Enzyme and Microbial Technology, 36*, 314–317. https://doi.org/10.1016/j.enzmictec.2004.09.002

Chen, K., Brennan, C., Brennan, M., Cheng, G., Li, L., Qin, Y., & Chen, H. (2024). The effect of *Dictyophora indusiata*, oats and Polygonatum kingianum on the physicochemical properties and in vitro digestion of pizza crust. *International Journal of Food Science & Technology, 59*, 785–796. https://doi.org/10.1111/ijfs.16834

Chen, Y., Ye, R., Yin, L., & Zhang, N. (2014). Novel blasting extrusion processing improved the physicochemical properties of soluble dietary fiber from soybean residue and *in vivo* evaluation. *Journal of Food Engineering, 120*, 1–8. https://doi.org/10.1016/j.jfoodeng.2013.07.011

Gu, M., Fang, H., Gao, Y., Su, T., Niu, Y., & Yu, L. (2020). Characterization of enzymatic modified soluble dietary fiber from tomato peels with high release of lycopene. *Food Hydrocolloids, 99*, Article 105321. https://doi.org/10.1016/j.foodhyd.2019.105321

Hua, Y., Yang, B., Tang, J., Ma, Z., Gao, Q., & Zhao, M. (2012). Structural analysis of water-soluble polysaccharides in the fruiting body of *Dictyophora indusiata* and their in vivo antioxidant activities. *Carbohydrate Polymers, 87*, 343–347. https://doi.org/10.1016/j.carbpol.2011.07.056

Huang, J., Liao, J., Qi, J., Jiang, W., & Yang, X. (2021). Structural and physicochemical properties of pectin-rich dietary fiber prepared from citrus peel. *Food Hydrocolloids, 110*, Article 106140. https://doi.org/10.1016/j.foodhyd.2020.106140

Huang, Y. L., Ma, Y. S., Tsai, Y. H., & Chang, S. K. C. (2019). *In vitro* hypoglycemic, cholesterol-lowering and fermentation capacities of fiber-rich orange pomace as affected by extrusion. *International Journal of Biological Macromolecules, 124*, 796–801. https://doi.org/10.1016/j.ijbiomac.2018.11.249

Jiang, C., Wang, R., Liu, X., Wang, J., Zheng, X., & Zuo, F. (2022). Effect of particle size on physicochemical properties and in vitro hypoglycemic ability of insoluble dietary Fiber from corn bran. *Frontiers in Nutrition, 9*. https://doi.org/10.3389/fnut.2022.951821

Jiang, W., Han, G., Zhou, C., Gao, S., Zhang, Y., Li, M., … Via, B. (2017). The degradation of lignin, cellulose, and hemicellulose in Kenaf Bast under different pressures using steam explosion treatment. *Journal of Wood Chemistry and Technology, 37*, 359–368. https://doi.org/10.1080/02773813.2017.1303514

Johar, N., Ahmad, I., & Dufresne, A. (2012). Extraction, preparation and characterization of cellulose fibres and nanocrystals from rice husk. *Industrial Crops and Products, 37*, 93–99. https://doi.org/10.1016/j.indcrop.2011.12.016

Khawas, P., & Deka, S. C. (2016). Isolation and characterization of cellulose nanofibers from culinary banana peel using high-intensity ultrasonication combined with chemical treatment. *Carbohydrate Polymers, 137*, 608–616. https://doi.org/10.1016/j.carbpol.2015.11.020

Kong, F., Wang, L., Gao, H., & Chen, H. (2020). Process of steam explosion assisted superfine grinding on particle size, chemical composition and physico-chemical properties of wheat bran powder. *Powder Technology, 371*, 154–160. https://doi.org/10.1016/j.powtec.2020.05.067

Li, J., Henriksson, G., & Gellerstedt, G. (2007). Lignin depolymerization/repolymerization and its critical role for delignification of aspen wood by steam explosion. *Bioresource Technology, 98*, 3061–3068. https://doi.org/10.1016/j.biortech.2006.10.018

Liao, W., Luo, Z., Liu, D., Ning, Z., Yang, J., & Ren, J. (2015). Structure characterization of a novel polysaccharide from Dictyophora indusiata and its macrophage immunomodulatory activities. *Journal of Agricultural and Food Chemistry, 63*, 535–544. https://doi.org/10.1021/jf504677r

Liu, X., Suo, K., Wang, P., Li, X., Hao, L., Zhu, J., Yi, J., Kang, Q., Huang, J., & Lu, J. (2021). Modification of wheat bran insoluble and soluble dietary fibers with snail enzyme. *Food Science and Human Wellness, 10*, 356–361. https://doi.org/10.1016/j.fshw.2021.02.027

Liu, X. Y., Yu, H. Y., Liu, Y. Z., Qin, Z., Liu, H. M., Ma, Y. X., & Wang, X.-D. (2022). Isolation and structural characterization of cell wall polysaccharides from sesame kernel. *LWT, 163*, Article 113574. https://doi.org/10.1016/j.lwt.2022.113574

Liu, Y., Ao, H., Zheng, J. X., Liang, Y., & Ren, D. F. (2022). Improved functional properties of dietary fiber from *Rosa roxburghii* Tratt residue by steam explosion. *Journal of Food Processing and Preservation, 46*, Article e16119. https://doi.org/10.1111/jfpp.16119

Liu, Y., Zhang, H., Yi, C., Quan, K., & Lin, B. (2021). Chemical composition, structure, physicochemical and functional properties of rice bran dietary fiber modified by cellulase treatment. *Food Chemistry, 342*, Article 128352. https://doi.org/10.1016/j.foodchem.2020.128352

Luo, X., Wang, Q., Fang, D., Zhuang, W., Chen, C., Jiang, W., & Zheng, Y. (2018). Modification of insoluble dietary fibers from bamboo shoot shell: Structural characterization and functional properties. *International Journal of Biological Macromolecules, 120*, 1461–1467. https://doi.org/10.1016/j.ijbiomac.2018.09.149

Ma, C., Ni, L., Guo, Z., Zeng, H., Wu, M., Zhang, M., & Zheng, B. (2022). Principle and application of steam explosion technology in modification of food fiber. *Foods, 11*, 3370. https://doi.org/10.3390/foods11213370

Ma, M., & Mu, T. (2016). Effects of extraction methods and particle size distribution on the structural, physicochemical, and functional properties of dietary fiber from deoiled cumin. *Food Chemistry, 194*, 237–246. https://doi.org/10.1016/j.foodchem.2015.07.095

Ouyang, H., Guo, B., Hu, Y., Li, L., Jiang, Z., Li, Q., Ni, H., Li, Z., & Zheng, M. (2023). Effect of ultra-high pressure treatment on structural and functional properties of dietary fiber from pomelo fruitlets. *Food Bioscience, 52*, Article 102436. https://doi.org/10.1016/j.fbio.2023.102436

Pan, L., Wang, L., Zhang, F., Zhang, Y., & Zheng, B. (2023). Structural characterization and bifidogenic activity of polysaccharide from Dictyophora indusiata. *Food Bioscience, 51*, Article 102297. https://doi.org/10.1016/j.fbio.2022.102297

Ren, F., Feng, Y., Zhang, H., & Wang, J. (2021). Effects of modification methods on microstructural and physicochemical characteristics of defatted rice bran dietary fiber. *LWT, 151*, Article 112161. https://doi.org/10.1016/j.lwt.2021.112161

Shen, M., Ge, Y., Kang, Z., Quan, Z., Wang, J., Xiao, J., … Cao, L. (2019). Yield and physicochemical properties of soluble dietary Fiber extracted from untreated and steam explosion-treated black soybean Hull. *Journal of Chemistry, 2019*, Article e9736479. https://doi.org/10.1155/2019/9736479

Shen, M., Weihao, W., & Cao, L. (2020). Soluble dietary fibers from black soybean hulls: Physical and enzymatic modification, structure, physical properties, and cholesterol binding capacity. *Journal of Food Science, 85*, 1668–1674. https://doi.org/10.1111/1750-3841.15133

Tang, X., Wang, Z., Zheng, J., Kan, J., Chen, G., & Du, M. (2023). Physicochemical, structure properties and in vitro hypoglycemic activity of soluble dietary fiber from adlay (Coix lachryma-jobi L. var. ma-yuen Stapf) bran treated by steam explosion. *Frontiers in Nutrition, 10*. https://doi.org/10.3389/fnut.2023.1124012

Tanpichai, S., Witayakran, S., & Boonmahitthisud, A. (2019). Study on structural and thermal properties of cellulose microfibers isolated from pineapple leaves using steam explosion. *Journal of Environmental Chemical Engineering, 7*, Article 102836. https://doi.org/10.1016/j.jece.2018.102836

Wang, C., Lin, M., Li, Y., & Guo, Z. (2024). Improvement of soluble dietary fiber quality in *Tremella fuciformis* stem by steam explosion technology: An evaluation of structure and function. *Food Chemistry, 437*, Article 137867. https://doi.org/10.1016/j.foodchem.2023.137867

Wang, C., Lin, M., Yang, Q., Fu, C., & Guo, Z. (2023). The principle of steam explosion technology and its application in food processing by-products. *Foods, 12*, 3307. https://doi.org/10.3390/foods12173307

Wang, Y., Shi, X., Yin, J., & Nie, S. (2018). Bioactive polysaccharide from edible *Dictyophora* spp.: Extraction, purification, structural features and bioactivities. *Bioactive Carbohydrates and Dietary Fibre, 14*, 25–32. https://doi.org/10.1016/j.bcdf.2017.07.008. A Festschrift in Honour of Professor Glyn O. Phillips at his 90th Birthday.

Wei, C., Ge, Y., Liu, D., Zhao, S., Wei, M., Jiliu, J., … Cao, L. (2022). Effects of high-temperature, high-pressure, and ultrasonic treatment on the physicochemical properties and structure of soluble dietary fibers of millet bran. *Frontiers in Nutrition, 8*. https://doi.org/10.3389/fnut.2021.820715

Wen, Y., Niu, M., Zhang, B., Zhao, S., & Xiong, S. (2017). Structural characteristics and functional properties of rice bran dietary fiber modified by enzymatic and enzyme-micronization treatments. *LWT, 75*, 344–351. https://doi.org/10.1016/j.lwt.2016.09.012

Wu, D.-T., Zhao, Y.-X., Yuan, Q., Wang, S., Gan, R.-Y., Hu, Y.-C., & Zou, L. (2022). Influence of ultrasound assisted metal-free Fenton reaction on the structural characteristic and immunostimulatory activity of a β-D-glucan isolated from *Dictyophora indusiata*. *International Journal of Biological Macromolecules, 220*, 97–108. https://doi.org/10.1016/j.ijbiomac.2022.08.058

Xi, H., Wang, A., Qin, W., Nie, M., Chen, Z., He, Y., Wang, L., Liu, L., Huang, Y., Wang, F., & Tong, L.-T. (2023). The structural and functional properties of dietary fibre extracts obtained from highland barley bran through different steam explosion-assisted treatments. *Food Chemistry, 406*, Article 135025. https://doi.org/10.1016/j.foodchem.2022.135025

Xing, Y., Zhou, Y., Kuang, C., Luo, K., Cheng, Y., Wang, X., & Wang, S. (2024). Structural, physicochemical and functional properties of dietary fibers from tea residue modified by steam explosion. *Frontiers in Sustainable Food Systems, 7*. https://doi.org/10.3389/fsufs.2023.1326102

Xu, Y., Cui, Y., Wang, X., Yue, F., Shan, Y., Liu, B., Zhou, Y., Yi, Y., & Lü, X. (2019). Purification, characterization and bioactivity of exopolysaccharides produced by *Lactobacillus plantarum* KX041. *International Journal of Biological Macromolecules, 128*, 480–492. https://doi.org/10.1016/j.ijbiomac.2019.01.117

Yan, K., Liu, J., Yan, W., Wang, Q., Huo, Y., Feng, S., … Xu, J. (2023). Effects of alkaline hydrogen peroxide and Cellulase modifications on the physicochemical and functional properties of *Forsythia suspensa* dietary Fiber. *Molecules, 28*, 7164. https://doi.org/10.3390/molecules28207164

Yang, C., Si, J., Chen, Y., Xie, J., Tian, S., Cheng, Y., Hu, X., & Yu, Q. (2022). Physicochemical structure and functional properties of soluble dietary fibers obtained by different modification methods from Mesona chinensis Benth. residue. *Food Research International, 157*, Article 111489. https://doi.org/10.1016/j.foodres.2022.111489

Yu, G., Bei, J., Zhao, J., Li, Q., & Cheng, C. (2018). Modification of carrot (*Daucus carota* Linn. var. Sativa Hoffm.) pomace insoluble dietary fiber with complex enzyme method, ultrafine comminution, and high hydrostatic pressure. *Food Chemistry, 257*, 333–340. https://doi.org/10.1016/j.foodchem.2018.03.037

Zhang, Z., Wang, L., Zheng, B., Zhang, Y., & Pan, L. (2024). *In vitro* digestive properties of *Dictyophora indusiata* polysaccharide by steam explosion pretreatment methods. *International Journal of Biological Macromolecules, 265*, Article 131116. https://doi.org/10.1016/j.ijbiomac.2024.131116

Zheng, Y., Wang, X., Tian, H., Li, Y., Shi, P., Guo, W., & Zhu, Q. (2021). Effect of four modification methods on adsorption capacities and in vitro hypoglycemic properties of millet bran dietary fibre. *Food Research International, 147*, Article 110565. https://doi.org/10.1016/j.foodres.2021.110565

Zhu, M., Huang, R., Wen, P., Song, Y., He, B., Tan, J., Hao, H., & Wang, H. (2021). Structural characterization and immunological activity of pectin polysaccharide from kiwano (*Cucumis metuliferus*) peels. *Carbohydrate Polymers, 254*, Article 117371. https://doi.org/10.1016/j.carbpol.2020.117371